ACS APPLIED MATERIALS & INTERFACES

www.acsami.org

Spotlight on Applications

The Rise of Silicon Phthalocyanine: From Organic Photovoltaics to Organic Thin Film Transistors

Benoît H. Lessard*

Cite This: *ACS Appl. Mater. Interfaces* 2021, 13, 31321−31330

Read Online

ACCESS | Metrics & More | Article Recommendations

ABSTRACT: Silicon phthalocyanines are emerging n-type semiconductors for use in organic photovoltaics (OPVs) and organic thin-film transistors (OTFTs). Their low synthetic complexity paired with their versatile axial group facilitates the fine-tuning of their chemical properties, solution properties and processing characteristics without significantly affecting their frontier orbital levels or their absorption properties. The crystal engineering and film forming characteristics of silicon phthalocyanine semiconductors can be tuned through appropriate axial group functionalization, therefore facilitating their integration into both OTFTs and OPVs by solution processing or vapor deposition. This Spotlight on Applications will discuss recent advances in the integration of this exciting class of phthalocyanine into OTFTs and OPVs and highlights their promising future.

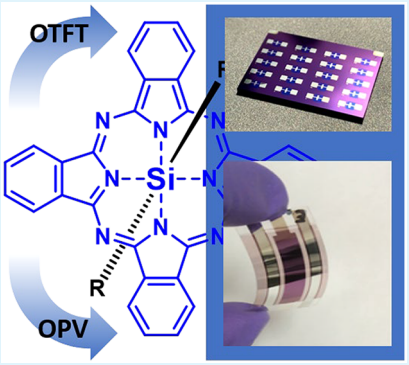

KEYWORDS: *silicon phthalocyanine, thin-film transistors, organic photovoltaics, n-type semiconductor, non-fullerene acceptors*

1. INTRODUCTION

Metal phthalocyanines (MPcs) are conjugated macrocycles that chelate a metal or metalloid inclusion. Since their discovery in the early 1900s, they have become a staple in the dye and pigment industry with some notable commercial derivatives such as Phthalo Blue (copper phthalocyanine, CuPc) or Phthalo Green (copper hexadecafluorophthalocyanine, F_{16}CuPc), which are commonly found in paints, colorants, inks, textiles, plastics, and more. Phthalocyanines are among the most important dyes with CuPc alone being the largest-volume colorant sold worldwide.[1] The chemistry is established, the precursors are abundant, and the industry is already producing them on the ton scale annually.

MPcs have also found their way into organic electronics due to their chemical stability and favorable optoelectronic properties. In 1985, the first example of a bilayer organic photovoltaic (OPV) device by Tang, when at Eastman Kodak, was based on CuPc paired with a perylene based derivative.[2] In fact MPcs have been used in a plethora of electronic applications including organic thin-film transistors (OTFTs),[3−6] OPVs,[7−9] organic light emitting diodes (OLEDs),[10] and sensors.[11,12] Our group has recently contributed to the development of MPc based devices through studying the effect of environment on OTFTs fabricated using different metal centers,[5] for the detection of single stranded DNA[13] and recently the detection and speciation of different cannabinoids.[14] We also screened a series of different MPcs to identify the effect of metal center and peripheral substitution on the selectivity of OTFT based cannabinoid sensors through quick solution based screening.[15]

Silicon phthalocyanines (R_2−SiPcs) are a class of MPc that has recently attracted interest from our group and several others. Due to the oxidation state of the silicon, we observe two axial bonds that are perpendicular to the aromatic macrocycle (Figure 1). These axial bonds serve as handles to impart solubility and tune surface and bulk properties without having a significant effect on the optical and electrochemical properties, a significant advantage over divalent MPcs such as CuPc or zinc phthalocyanine (ZnPc). Interestingly, R_2−SiPc derivatives appear to inherently behave as n-type semiconductors: they favor the transport of electrons over holes, which is uncommon for MPcs. The following spotlight will focus on the engineering of R_2−SiPc based electronic devices, mainly our work on OTFTs and OPVs, since 2014.

2. SYNTHESIS AND PROCESSING

The syntheses of R_2−SiPc derivatives have recently been reviewed by Mitra and Hartman,[30] and therefore only emphasis on derivatives for use in OPVs and OTFTs will be covered in this section. Most MPcs are synthesized by directly reacting phthalonitrile with the corresponding metal/metalloid precur-

Received: April 6, 2021
Accepted: June 17, 2021
Published: July 1, 2021

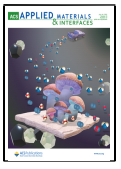

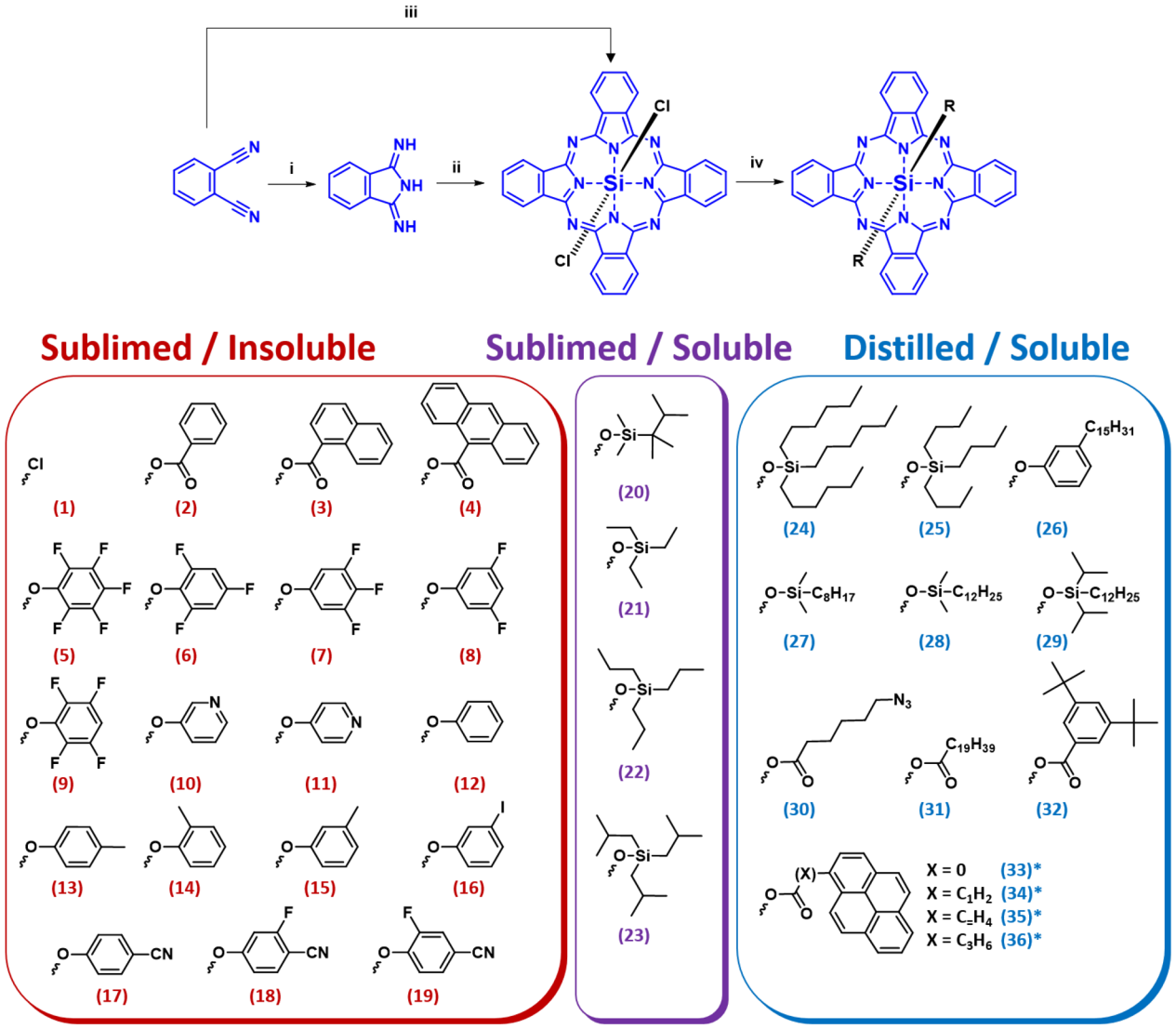

Figure 1. Synthetic routes in the preparation of bis-functional silicon phthalocyanines (R_2−SiPc) by either a two-step reaction (i and ii) through commercially available diiminoisoindoline (DIII) or a one-pot reaction (iii) directly from phthalonitrile using lithium bis(trimethylsilyl)amide etherate ($LiN(TMS)_2{\cdot}Et_2O$) leading to the formation of Cl_2−SiPc, which can then be converted to a library of R_2−SiPc derivatives through coupling with silanes, phenols, or carboxylic acids: **1** (Cl_2−SiPc);[16,17] **2** (PhCOO−SiPc);[18] **3** (NpCOO−SiPc);[18] **4** (AnCOO−SiPc);[18] **5** (F_{10}−SiPc);[16,17] **6** (246F−SiPc);[19] **7** (345F−SiPc);[19] **8** (35F−SiPc);[19] **9** (2356F−SiPc);[19] **10** (3Pyr−SiPc);[20] **11** (4Pyr−SiPc);[20] **12** (PhO−SiPc);[20] **13** (4MP−SiPc);[20] **14** (2MP−SiPc);[20] **15** (3MP−SiPc);[20] **16** (3I−SiPc);[21] **17** (CN−SiPc);[22] **18** (3FCN−SiPc);[22] **19** (2FCN−SiPc);[22] **20** (TTS−SiPc);[23] **21** (3ES−SiPc);[23] **22** (3PS−SiPc);[24] **23** (3tBS−SiPc);[23] **24** (3HS−SiPc);[25] **25** (3BS−SiPc);[25] **26** (PDP−SiPc);[25] **27** (*n*OS−SiPc);[23] **28** (*n*DS−SiPc);[23] **29** (tnDS-SiPc);[23] **30** (N3O−SiPc);[26] **31** (EACOO−SiPc);[27] **32** (35tBPhCOO−SiPc);[27] **33** (PyrCOO−SiPc);[28,29] **34** (PyrMCOO−SiPc);[28,29] **35** (PyrECOO−SiPc);[28,29] **36** (PyrPCOO−SiPc).[28,29] The R_2−SiPc derivatives are categorized as insoluble (<5 mg/mL), soluble (>5 mg/mL), sublimed (sublimation temperature < melting temperature), and/or distilled (sublimation temperature > melting temperature). *, SiPc with peripheral *tert*-butyl functionalization.

sor with high yield and purity. Unfortunately, when reacting phthalonitrile and silicon tetrachloride together, we obtain less than 1% **1** (Cl_2−SiPc).[18,31] The synthesis of other tetravalent MPcs such as germanium and tin are high yielding using this procedure, justifying our interest for their use in electronic devices, however without success.[25,32,33] The first respectable procedure for the synthesis of Cl_2−SiPc was reported in the 1930s with the use of diiminoisoindoline (DIII) with a yield of 71% (Figure 1).[34] The synthesis of DIII involves the constant bubbling of ammonia into a solution of phthalonitrile and sodium methoxide leading to a product that is hard to purify. While it is possible to use as crude or as a one-pot reaction,[35] this additional step makes the synthesis of **1** (Cl_2−SiPc) challenging. Only recently has this procedure been improved by Brusso and co-workers, where they eliminated the use of sodium metal and ammonia gas through the use of lithium bis(trimethylsilyl)-amide etherate ($LiN(TMS)_2{\cdot}Et_2O$), providing a straightforward route to synthesize **1** in high purity (Figure 1).[36] Compound **1** can then easily be functionalized through axial reactions such as halogen exchanges[37] or simple one-step coupling reactions with phenols,[21] silanes,[38] or carboxylic acids.[18] In some cases, it is preferred to first go through the di(hydroxyl) silicon phthalocyanine intermediate prior to functionalization with silanes.[25,38] The functionalization of the axial group provides a handle for fine-tuning the molecular stacking and solubility without significant modification (up to ≈0.5 eV) to the frontier molecular orbitals (Figure 2) of the R_2−SiPc itself. This molecular tuning is critical for OPV and OTFT design through

https://doi.org/10.1021/acsami.1c06060
ACS Appl. Mater. Interfaces 2021, 13, 31321−31330

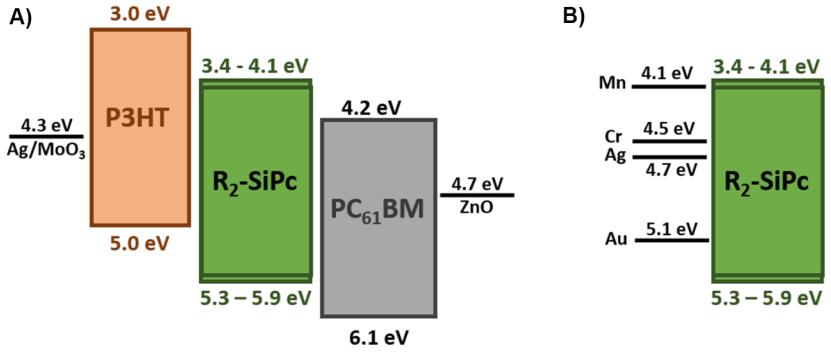

Figure 2. Characteristic band diagram for R_2−SiPcs in a typical (A) organic photovoltaic structure with poly(hexylthiophene) (P3HT) and phenyl-C_{61}-butyric acid methyl ester ($PC_{61}BM$) for comparison, as well as (B) in an organic thin-film transistor (OTFT) with the corresponding work function of metals and interlayers typically paired with R_2−SiPcs.

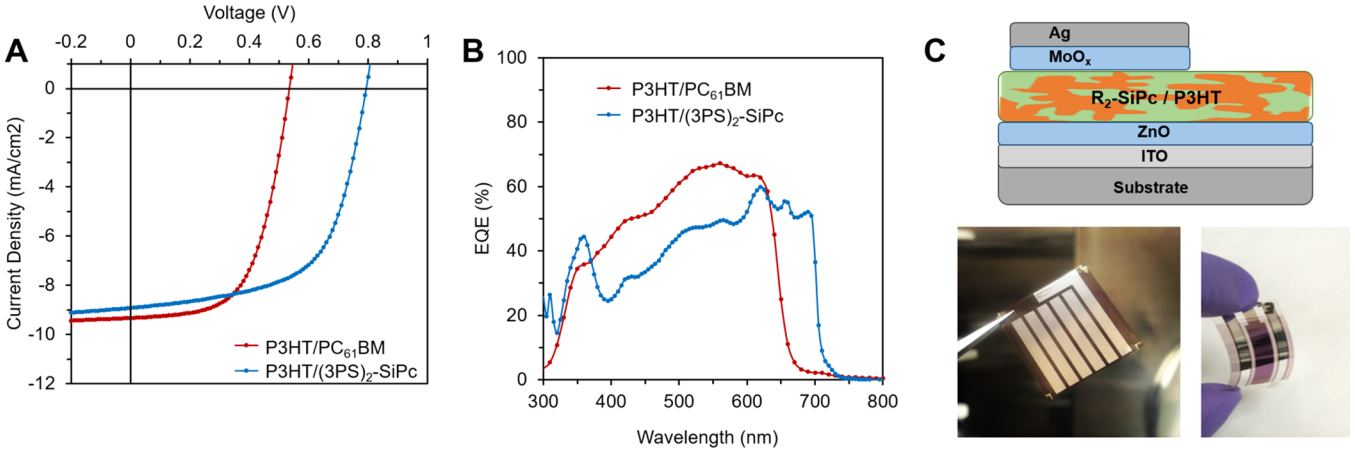

Figure 3. Characteristic P3HT/$PC_{61}BM$ and P3HT/**22** (3PS−SiPc) bulk heterojunction OPV. (A) J−V curves measured under 1000 W m^{-2} AM1.5G irradiation and (B) their respective EQE spectra. Panels A and B reprinted with permission from ref 24. Copyright 2021 The Royal Society of Chemistry. (C) schematic of an inverted OPV device structure with electrode interlayer and hole and electron transport layers. The two pictures are of typical OPVs containing R_2−SiPcs on glass and PET substrates.

engineering interactions between the R_2−SiPc and the surface or with other active materials.

3. SIPC BASED OPVS

OPVs represent an energy harvesting technology with low energy payback, ease of flexible integration, and potential for low-cost manufacturing. Recent advances in the field have shown tremendous improvements with power conversion efficiencies (PCEs) reaching >17%. Unfortunately, many of these record-breaking devices are based on materials which have negligible industrial potential due to excessive synthetic steps. It is critical to not only focus on device performance but also on material scale-up potential if we want this technology to be competitive or even viable. OPVs are based on the interaction between a donor molecule (or polymer) and an acceptor molecule (or polymer). Basic device performance can be characterized by the relationship between open circuit voltage (V_{OC}), the maximum voltage from an OPV when the net current through the cell is zero; the short circuit current per area (J_{SC}), which is the current through the solar cell when the voltage across the solar cell is zero; and the fill factor (FF), which is an ideality factor representing the "squareness" of the plot. The greater the V_{OC}, J_{SC}, and FF, the greater the overall PCE. The external quantum efficiency (EQE) plot demonstrates the photoconversion efficiency as a function of the wavelength of absorbed light; these plots often mirror the absorption profile of the OPV active layer with the area under the curve equal to the J_{SC}. A typical density−voltage (J−V) curve and EQE plot can be found in Figure 3A,B, respectively. Several recent reviews outline the working principles of OPVs in greater detail.[39,40]

In 1983 R_2−SiPc derivatives made their first appearance in single layer OPVs with basic electrical characterization.[41] Fast-forward to 2009 where Honda et al. demonstrated that **24** (3HS−SiPc) can act as an effective ternary additive in a poly(3-hexylthiophene):phenyl-C_{61}-butyric acid methyl ester (P3HT:$PC_{61}BM$) bulk heterojunction (BHJ) OPV device providing 20% increase in PCE due to the increased J_{SC} from the additional absorption of the R_2−SiPc at 685 nm.[42] Compound **24** is effective at low loadings (<10 wt %) because it migrates to the P3HT:$PC_{61}BM$ interface, facilitating the cascade energy transfer.[43−45] Since then, several studies have explored variations in the axial groups in attempts to improve morphology or induce secondary improvements. For example, Xu et al. designed an asymmetric R_2−SiPc additive with hexyl groups compatible with the P3HT and a benzyl group that are compatible with the $PC_{61}BM$ leading a 30% increase in PCE compared to the binary BHJ OPV device.[46] Ke et al. synthesized pyrene-functional R_2−SiPc derivatives (**33**−**36**) to expand the UV absorption of the ternary additive leading to an increase in J_{SC} and V_{OC}.[28,29] Our group reported the first multifunctional ternary additive (**30**) which produced additional photogeneration due to the R_2−SiPc chromophore, while simultaneously

https://doi.org/10.1021/acsami.1c06060
ACS Appl. Mater. Interfaces 2021, 13, 31321−31330

providing device stability due to the cross-linking of the azide groups with the $PC_{61}BM$.[26] Bender and co-workers reported that even small changes in molecular structure of the R_2−SiPc such as *n*-butylsilane (**25**) versus *n*-hexylsilane groups (**24**) can have significant effects on the crystallization and the ultimate BHJ OPV performance.[25,38] Building on this observation, our group recently investigated a series of R_2−SiPc derivatives with varying silane functionalities (Figure 4) and found that when the

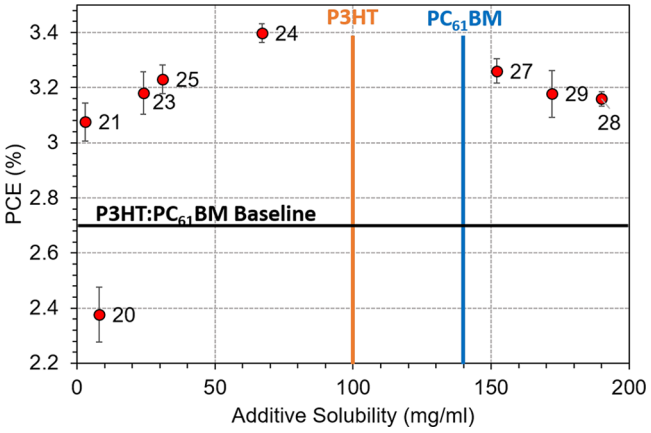

Figure 4. PCE versus R_2−SiPc ternary additive solubility in dichlorobenzene for P3HT:$PC_{61}BM$:R_2−SiPc ternary BHJ OPV devices. Black line represents the binary baseline, while the orange and blue lines represent the solubilities of P3HT and $PC_{61}BM$, respectively. The numbers correspond to choice of R_2-SiPc as identified in Figure 1. Adapted with permission from ref 23. Copyright 2020 American Chemical Society.

solubility of the ternary additive approached that of the P3HT, the greatest PCE improvement was observed.[23] We surmise this compatibility leads to more dye at the interface during drying leading to optimal device performance.[23] Recently we synthesized bisfunctional tin phthalocyanines (R_2−SnPcs) with identical axial functional groups and found that the corresponding R_2−SnPcs were detrimental to OPV performance, which we concluded was due to the photoinstability of the R_2−SnPcs in thin films.[33] While negative, these results further justify the interest in R_2−SiPcs derivatives for use in OPVs.

In addition to their use as ternary additives, R_2−SiPcs have recently been considered as a non-fullerene acceptor (NFA) in a binary device. Bender and co-workers first reported the use of **24** (3HS−SiPc) and **25** (3BS−SiPc) as NFAs with P3HT leading to PCEs of <1%.[38] Zysman-Colman et al. also reported **31** (EACOO−SiPc)[27] and **32** (35tBPhCOO−SiPc)[27] as NFAs when paired with P3HT (PCE < 0.5%) or with poly[[4,8-bis[(2-ethylhexyl)oxy]benzo[1,2-*b*:4,5-*b*′]dithiophene-2,6-diyl][3-fluoro-2-[(2-ethylhexyl)carbonyl]thieno[3,4-*b*]thiophenediyl]] (PTB7) leading to a PCE of 0.27% when using **31** and a PCE of 2.67% when using **32**. Recently our group optimized the P3HT:**25** BHJ inverted device which led to a PCE of 3.6% (V_{OC} = 0.76 V) outperforming the P3HT:$PC_{61}BM$ baselines.[47] We have also reported the use of P3HT:**22** (3PS−SiPc) BHJ inverted device, which led to a PCE of 4.3% (V_{OC} = 0.79 V) also outperforming the P3HT:$PC_{61}BM$ baselines (Figure 3).[24] Additionally, when **25** was paired with poly[(2,6-(4,8-bis(5-(2-ethylhexyl)thiophen-2-yl)benzo[1,2-*b*:4,5-*b*′]-dithiophene))-*alt*-(5,5-(1′,3′-di-2-thienyl-5′,7′-bis(2-ethylhexyl)benzo[1′,2′-*c*:4′,5′-*c*′]dithiophene-4,8-dione)] (PBDB-T), it led to an exceptionally high V_{OC} of 1.10 V (PCE = 3.4%),[47] and with PTB7, which also led a high V_{OC} of 1.07 V (PCE = 3.8%).[48] However, in both cases the FF and J_{SC} were not as high as the corresponding $PC_{61}BM$ baselines. We found this was due to the fast crystallization of **25**, leading to unfavorable film morphology when blended with the polymer. AFM and synchrotron scanning transmission X-ray microscopy (STXM) studies have demonstrated that when blended with P3HT, typical R_2−SiPc domains are significantly larger and the composition is less uniform throughout the film compared to when using $PC_{61}BM$.[24] Another important consideration is the synthetic complexity (SC) and true scale-up potential of the active materials used in OPVs. SC has recently been calculated as a function of weighted parameters such as synthetic steps, the reciprocal of the cumulative synthetic yield, the number of unit operations, the number of column chromatography purification steps, and the number of highly hazardous chemicals that are necessary. The lower the SC, the greater the potential for large-scale synthesis and industrial uptake. R_2−SiPc s[24] have been calculated to have an SC, which is four to six times smaller than common NFAs such as O-IDTBR,[49] ITIC,[50] and Y6.[51] This is not surprising as MPcs, such as R_2−SiPcs, are commercial dyes produced on the ton scale annually, further justifying the continued investigation into their use in OPVs.

Preliminary planar heterojunction (PHJ) OPVs by physical vapor deposition of **1** (Cl_2−SiPc), **5** (F_{10}−SiPc), **6** (246F−SiPc), **7** (345F−SiPc), **8** (35F−SiPc), or **9** (2356F−SiPc), as both the acceptors when paired with *α*-sexithiophene (*α*-6T) or pentacene and the donor when paired with fullerene, have led to decent V_{OC}, approaching 0.95 V, and PCE as high as 1.8%.[16,19] Compound **22** (3PS−SiPc), which was integrated into a BHJ

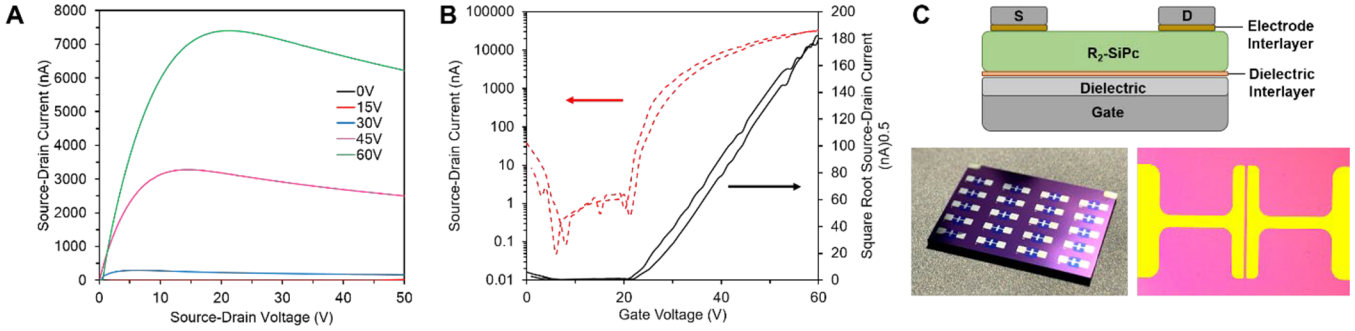

Figure 5. Characteristic OTFTs. (A) Output curves at different gate voltages and (B) transfer curve for **5** (F_{10}−SiPc). Panels A and B adapted with permission from ref 66. Copyright 2020 American Chemical Society. (C) Schematic of a bottom-gate top-contact OTFT with electrode interlayer and dielectric interlayer modification. The two pictures are of typical OTFTs with microscope image of actual channel.

https://doi.org/10.1021/acsami.1c06060
ACS Appl. Mater. Interfaces 2021, 13, 31321−31330

OPV due to its high solubility, was also integrated into a PHJ OPV configuration due to its ability to be sublimed (Figure 1), leading to a modest PCE of 0.7% (V_{OC} = 0.62 V) when paired with α-6T as a small-molecule donor.[24] Recently, we reported the combination of solution-processed P3HT or PCDTBT followed by the evaporation of either **6** (246F−SiPc) or **7** (345F−SiPc), leading to a hybrid-processed OPV device with high V_{OC} and PCE of ≈1%.[52] It is also important to note that while the devices were not groundbreaking, with this hybrid-processed structure the R_2−SiPc based devices outperformed the fullerene controls (P3HT/C_{60}), further suggesting that R_2−SiPc derivatives are good substitutes for fullerenes.[52] Finally, R_2−SiPc derivatives were also found to be effective sensitizing dyes when used in dye-sensitized solar cells,[53] but no follow-up studies have been reported.

4. R_2−SIPC BASED OTFTS

OTFTs are logic gate operators, or electrical switches, fabricated using carbon based semiconductors. From activating the pixels in flexible displays to electronic skin and wearable sensors, the versatility and need for high-performing OTFTs is becoming increasingly evident. These three electrode devices rely on an applied gate voltage which polarizes a dielectric material, populating the semiconductor interface with carriers, either holes for p-type or electrons for n-type, leading to current being measured across a source and drain electrode (Figure 5C). Historically, conjugated molecules have more easily transported holes than electrons and therefore the search for stable, high n-type performing materials has been of great interest to the field.[4,54,55] Recently, some promising materials have emerged with either high electron mobility, (μ_e) or low threshold voltages (V_T) and sometimes both. Among these materials, there are conjugated polymers,[56,57] single walled carbon nanotubes,[58−60] and small molecules. Small molecules have the advantage of being often easier to purify with less batch-to-batch variation compared to polymers with variable molecular weights and dispersity challenges. Among the most promising small-molecule families are oligothiophenes, isoindigo based, anthracene based, naphthalene tetracarboxylic diimide (NDI), and perylene diimide (PDI) molecules.[61] While the majority of these derivatives have μ_e = 0.001−1.0 $cm^2 V^{-1} s^{-1}$ (V_T between 0 and 50 V), there are some exceptions, for example certain isoindigo based derivatives[62,63] have reported $\mu_e \approx 6$ to 12 $cm^2 V^{-1} s^{-1}$ (V_T between 9 and 12 V) for and some oligothiophene based molecules[64,65] have also been characterized with a $\mu_e \approx 3$−5 $cm^2 V^{-1} s^{-1}$ (V_T between −1.4 and −14 V). In most of these cases the chemistry is multistep and challenging to scale up. The following section highlights the operation, fabrication, and challenges with R_2−SiPc OTFTs.

The first example of OTFTs fabricated using R_2−SiPcs were reported by our group using **2** (PhCOO−SiPc), **3** (NpCOO−SiPc), and **4** (AnCOO−SiPc).[18] In devices, the R_2−SiPc exhibited μ_e up to ≈0.01 $cm^2 V^{-1} s^{-1}$, which was several orders of magnitude greater than the hole mobility (μ_h), even when using Au electrodes that have a work function that is more favorably matched to the highest occupied molecular orbital (HOMO) of the R_2−SiPc derivatives. We found that the larger the aromatic pendant group, the larger the π−π distances between aromatic macrocycles in the single crystals, which resulted in a reduction in μ_e.[18] Additionally, processing factors such as choice of surface functionalization, substrate temperature during deposition and deposition rate led to an improvement in μ_e by over 3 orders of magnitude.[18] Following this study we explored the use of **5** (F_{10}−SiPc), **6** (246F−SiPc), and **7** (345F−SiPc) and compared them with **1** (Cl_2−SiPc). Compound **5** (F_{10}−SiPc) exhibited record μ_e = 0.54 cm/(V s)^2, which is an order of magnitude greater than what we obtained using F_{16}−CuPc and almost double what others have obtained when applying different surface engineering.[17] Compound **5** has been characterized with greater single crystal packing and π−π interactions, likely aiding in charge transport.[16,19] While the high μ_e is promising, the devices suffered from high contact resistance, high V_T, and air instability. Therefore, we designed new OTFTs using **5** (and other R_2−SiPcs) by changing the device structure from bottom-gate bottom-contact (BGBC) to bottom-gate top-contact (BGTC) and changed the electrode metal to include different interlayers between the electrodes and the semiconductor (Figure 5C).[67] We found that the use of manganese (Mn), which tuned the electrode work function to match the lowest occupied molecular orbital (LUMO) of the R_2−SiPc, paired with BGTC configuration, reducing the contact resistance and decreasing the V_T from 23.5 to 7.8 V.[67] Moving through the integration of various R_2−SiPc derivatives, we observed significant differences in V_T and decided to probe further. In attempts to better understand the effect of the R_2−SiPc axial group selection on device performance, we looked at 11 different vapor-deposited R_2−SiPcs and integrated them into OTFTs under identical processing conditions for comparison.[66] We found that the smallest change, such as the location of a methyl group, or the number of fluorines in the phenoxy group can result in significant changes in the thin-film morphology and device performance. The most striking correlation appeared to be between the Hammett parameter, or electron donating/withdrawing character of the R_2−SiPc axial group, and the resulting device V_T: as the Hammett parameter increases, the device V_T decreases (Figure 6).[66] To further investigate this

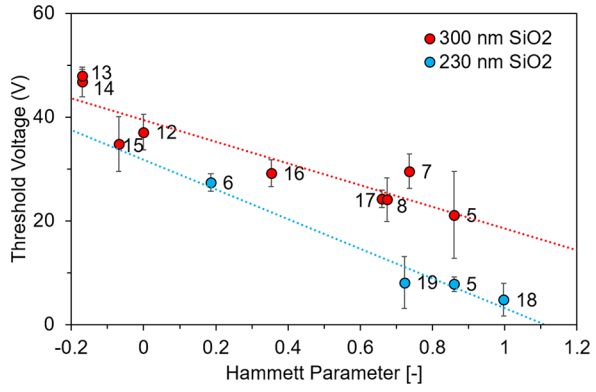

Figure 6. V_T of OTFTs as a function of Hammett parameter of axial pendant groups for R_2−SiPcs. Devices were fabricated using 230 nm thick (blue circles) and 300 nm thick (red circles) OTS-modified SiO_2 (dielectric interlayer). The numbers correspond to choice of R_2-SiPc as identified in Figure 1. Adapted with permission from ref 22. Copyright 2021 American Chemical Society. Data also from refs 67 and 66.

observation, we synthesized a series of cyano-functional R_2−SiPcs: **17** (CN−SiPc), **18** (3FCN−SiPc), and **19** (2FCN−SiPc).[22] The resulting OTFTs made with these cyano-functional R_2−SiPc derivatives matched the trend, even when using different oxide thicknesses as dielectric (Figure 6). Devices made with **18** led to V_Ts as low as ≈2 V with modest $\mu_e = 5 \times 10^{-4}$ $cm^2 V^{-1} s^{-1}$. While this correlation between molecular structure and V_T is helpful, we have found that predicting the μ_e

https://doi.org/10.1021/acsami.1c06060
ACS Appl. Mater. Interfaces 2021, 13, 31321−31330

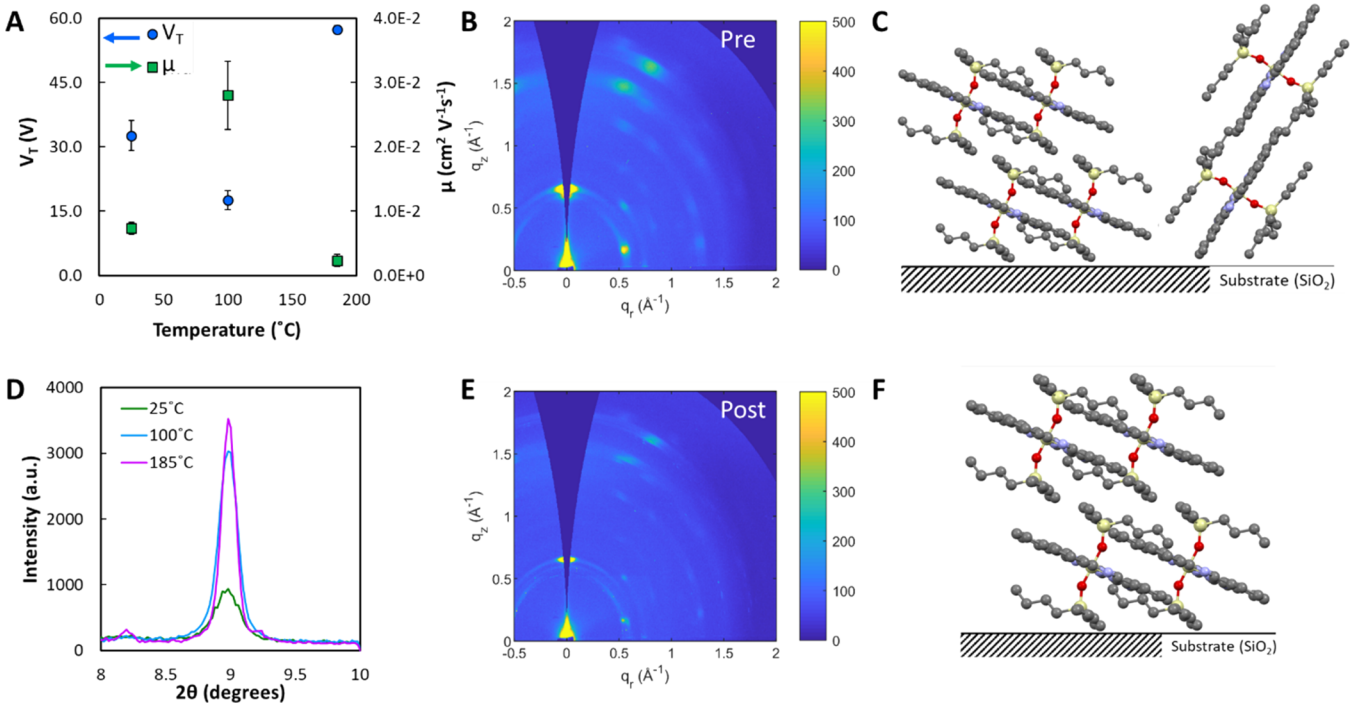

Figure 7. Change in (A) μ_e and V_T for **25** OTFTs annealed at 25, 100, and 185 °C. (D) X-ray diffraction pattern of films. 2D scattering patterns for films annealed at (B) 25 °C and $\alpha = 0.02°$ and (E) 185 °C and $\alpha = 0.03°$ determined by GIWAXS. Diagram of (C) a combination of pseudoface on and pseudoedge on orientations, and (F) pseudoface on orientation to the substrate determined by GIWAXS. Reprinted with permission from ref 69. Copyright 2020 American Chemical Society.

of thin-film devices is more difficult due to a wide range of possible grain structures in R_2−SiPc films. Castet's and Muccioli's groups in collaboration with our group have been working on predicting the charge transport properties of R_2−SiPcs by means of kinetic Monte Carlo simulations based on experimental single crystal structures resolved by X-ray diffraction techniques.[68] The simulations also provide evidence of charge transport dimensionality, further justifying the need to study molecular alignment at the dielectric and semiconductor interface. For example, we employed grazing-incidence wide-angle X-ray scattering (GIWAXS) to study thin films of **5** (F_{10}−SiPc) and **3** (NpCOO−SiPc) on SiO_2 modified by an octyltrichlorosilane (OTS) self-assembled monolayer (the same dielectric surface as OTFT devices) and found that **5** exhibited mixed orientations with a majority of molecules exhibiting a pseudoface on orientation while **3** exhibited pseudoedge on orientation with relatively smaller π−π distances.[66] While material **3** possessed a pseudo edge-on orientation and smaller π−π distances, it performed worse in devices with a lower μ_e and greater V_T. This result, however, could be explained by density functional theory (DFT) modeling which identified a relatively high intermolecular electronic coupling parallel to the substrate for **5**, while **3** exhibited relatively low intermolecular electronic coupling.[66] These studies suggest that the performance of R_2−SiPc based OTFT performance can be partially predicted by DFT modeling and that these design rules will aid in the development of new high-performing derivatives.

The promise of low manufacturing cost and large-area production drives the desire to process these materials from solution. Due to the axial groups on the R_2−SiPc, it is possible to make the derivatives soluble as discussed in the OPV section. Therefore, our group was the first to implement solution-processed **24** (3HS−SiPc) and **25** (3BS−SiPc) based OTFTs with $\mu_e \approx 1.6 \times 10^{-4}$ cm^2 V^{-1} s^{-1} and V_T of 22 V.[32] We found that the crystallization and film morphology were heavily dependent on choice of solvent, processing temperature, and processing conditions. When studying the interface, we found that molecular orientation of the semiconductor at the dielectric interface changed between edge-on and face-on, depending on the processing conditions. For example, GIWAXS demonstrated that the annealing temperature and spin speed/time had a significant effect on the thin-film morphology of **25** leading to improvement in OTFT performance with $\mu_e \approx 4.2 \times 10^{-2}$ cm^2 V^{-1} s^{-1} and V_T of 17 V (Figure 7).[69] We also integrated **20**, **21**, **23**, **24**, **25**, **27**, **28**, and **29** into solution-processed OTFTs and found that the choice of axial group has a significant effect on film formation due to different crystallization drivers, leading to significant differences in devices performance.[69] These results suggest that choice of axial groups as well as processing conditions are paramount to improved film formation and ultimate device performance.

5. OTHER APPLICATIONS

Beyond OPVs and OTFTs, R_2−SiPcs have found their way into a plethora of applications. R_2−SiPcs have a strong molar extinction coefficient and an incredibly small Stokes shift (<4 nm), which makes them interesting for various solid state applications involving the generation or absorption of red/near-IR (NIR) light. For example, Pearson et al. integrated **5** (F_{10}−SiPc) into solution-processed organic light emitting diodes (OLEDs) as red/NIR fluorescent emitters with 20 nm full width at half-maximum emission.[70] Zysman-Colman et al. also reported the use of **31** (EACOO−SiPc) and **32** (35tBPhCOO−SiPc) as emitters in OLEDs.[27] Plint et al. employed **1** (Cl_2−SiPc) as hole transport layer in some basic

https://doi.org/10.1021/acsami.1c06060
ACS Appl. Mater. Interfaces 2021, 13, 31321−31330

ALQ_3 based green OLEDs and compared it to other MPcs.[71] Lalevée and co-workers demonstrated that R_2−SiPcs can be used as laser absorbing dyes for NIR based photopolymerization of methacrylic monomers.[72,73]

While beyond the scope of this review, which has focused on solid state thin-film electronic devices, it is important to note that R_2−SiPcs have had an excellent track record for use in light based medical applications. Water-soluble R_2−SiPcs have been used as potential candidates for photodynamic therapies,[74−77] antibacterial or antifungal agents,[78,79] in vitro and in vivo bioimaging,[80,81] and more. These examples suggest the exciting potential for the use of R_2−SiPc in a crossover between solid state electronic devices and biological/medical applications.

6. CONCLUSION AND OUTLOOK

R_2−SiPcs have undoubtedly proven themselves as molecules worthy of further study as semiconductors in organic electronics. Their low synthetic complexity means they can be synthesized on an industrial scale like other MPcs currently found in the dye and pigment industry. Unlike other MPcs, R_2−SiPcs can easily be fine-tuned through axial functionalization, which makes them versatile in terms of attaining ideal film formation and processing conditions. For example, when solution processing by spin coating versus screen printing or blade coating, the ink requirements are different and therefore changing the axial group from propyl to hexyl (for example) will change solution properties such as viscosity and film forming properties such as enthalpy of crystallization which can be used to match the type of processing technique. The engineering of bulk properties as well as surface and interfacial interactions can be tuned with relative ease, making them compatible with various substrate chemistries and processes. Other semiconductors may suffer from complex chemistry to implement such changes or this implementation cannot be made without simultaneously affecting the frontier orbitals resulting in changes in optical or electrical properties, which again is not the case with R_2−SiPcs.

However, much work is required to make these derivatives competitive with existing high-performing NFAs for OPVs and n-type semiconductors for OTFTs. According to me, the greatest challenge for use as an NFA is to find a matching conjugated polymer. Most low band gap polymers are not suitable because of their mismatch in frontier orbital levels compared to that of R_2−SiPc. Furthermore, the R_2−SiPcs tend to crystallize very quickly while a lot of the high-performing, low band gap polymers are amorphous. Therefore, being able to match the crystallization of R_2−SiPc with an appropriate polymer that also crystallizes quickly would be ideal. For OTFTs, the greatest challenge is air stability. All R_2−SiPcs mentioned in this text are not air stable; however, modification of the peripheral groups around the R_2−SiPc macrocycle can drop the LUMO level, resulting in increased air stability. The chemistry is challenging, but the reward is obvious. If we can engineer an air stable R_2−SiPc macrocycle without giving up the axial groups for fine chemical tuning, then we should have a champion n-type semiconductor. Needless to say, these are the directions our group is currently investigating, and we invite others to join us and collaborate on the development of these exciting molecules.

AUTHOR INFORMATION

Corresponding Author

Benoît H. Lessard − *Department of Chemical and Biological Engineering and School of Electrical Engineering and Computer Science, University of Ottawa, Ottawa, Ontario, Canada K1N 6N5;* orcid.org/0000-0002-9863-7039; Email: benoit.lessard@uottawa.ca

Complete contact information is available at: https://pubs.acs.org/10.1021/acsami.1c06060

Notes

The author declares no competing financial interest.

ACKNOWLEDGMENTS

The Natural Sciences and Engineering Research Council of Canada (Grant No. RGPIN-2020-04079) is acknowledged for financial support. To my daughters, Eveline and Milaine for being good sleepers and giving me the opportunity to write this article during a pandemic.

REFERENCES

(1) Gregory, P. Industrial Applications of Phthalocyanines. *J. Porphyrins Phthalocyanines* **2000**, *4* (4), 432−437.

(2) Tang, C. Two-Layer Organic Photovoltaic Cell. *Appl. Phys. Lett.* **1986**, *48* (2), 183−185.

(3) Li, L.; Tang, Q.; Li, H.; Hu, W.; Yang, X.; Shuai, Z.; Liu, Y.; Zhu, D. Organic Thin-Film Transistors of Phthalocyanines. *Pure Appl. Chem.* **2008**, *80* (11), 2231−2240.

(4) Melville, O. A. O.; Lessard, B. H. B. H.; Bender, T. P. T. P. Phthalocyanine Based Organic Thin-Film Transistors: A Review of Recent Advances. *ACS Appl. Mater. Interfaces* **2015**, *7* (24), 13105−13118.

(5) Boileau, N. T.; Cranston, R.; Mirka, B.; Melville, O. A.; Lessard, B. H. Metal Phthalocyanine Organic Thin-Film Transistors: Changes in Electrical Performance and Stability in Response to Temperature and Environment. *RSC Adv.* **2019**, *9* (37), 21478−21485.

(6) Zhou, W.; Yutronkie, N. J.; Lessard, B. H.; Brusso, J. L. From Chemical Curiosity to Versatile Building Blocks: Unmasking the Hidden Potential of Main-Group Phthalocyanines in Organic Field-Effect Transistors. *Mater. Adv.* **2021**, *2*, 165−185.

(7) de la Torre, G.; Claessens, C. G.; Torres, T. Phthalocyanines: Old Dyes, New Materials. Putting Color in Nanotechnology. *Chem. Commun.* **2007**, No. 20, 2000−2015.

(8) de la Torre, G.; Bottari, G.; Torres, T. Phthalocyanines and Subphthalocyanines: Perfect Partners for Fullerenes and Carbon Nanotubes in Molecular Photovoltaics. *Adv. Energy Mater.* **2017**, *7*, 1601700.

(9) Grant, T. M.; Josey, D. S.; Sampson, K. L.; Mudigonda, T.; Bender, T. P.; Lessard, B. H. Boron Subphthalocyanines and Silicon Phthalocyanines for Use as Active Materials in Organic Photovoltaics. *Chem. Rec.* **2019**, *19* (6), 1093−1112.

(10) Hohnholz, D.; Steinbrecher, S.; Hanack, M. Applications of Phthalocyanines in Organic Light Emitting Devices. *J. Mol. Struct.* **2000**, *521* (1), 231−237.

(11) Bouvet, M. Phthalocyanine-Based Field-Effect Transistors as Gas Sensors. *Anal. Bioanal. Chem.* **2005**, *384* (2), 366−373.

(12) Bouvet, M.; Guillaud, G.; Leroy, A.; Maillard, A.; Spirkovitch, S.; Tournilhac, F.-G. Phthalocyanine-Based Field-Effect Transistor as Ozone Sensor. *Sens. Actuators, B* **2001**, *73* (1), 63−70.

(13) Boileau, N. T.; Melville, O. A.; Mirka, B.; Cranston, R.; Lessard, B. H. P and N Type Copper Phthalocyanines as Effective Semiconductors in Organic Thin-Film Transistor Based DNA Biosensors at Elevated Temperatures. *RSC Adv.* **2019**, *9* (4), 2133−2142.

(14) Comeau, Z. J.; Boileau, N.; Lee, T.; Melville, O. A.; Rice, N.; Troung, Y.; Harris, C. S.; Lessard, B. H.; Shuhendler, A. J. On-The-Spot Detection and Speciation of Cannabinoids Using Organic Thin Film Transistors. *ACS Sensors* **2019**, *4* (10), 2706−2715.

(15) Comeau, Z. J.; Facey, G. A.; Harris, C. S.; Shuhendler, A. J.; Lessard, B. H. Engineering Cannabinoid Sensors through Solution-Based Screening of Phthalocyanines. *ACS Appl. Mater. Interfaces* **2020**, *12* (45), 50692−50702.

(16) Lessard, B. H.; White, R. T.; Al-Amar, M.; Plint, T.; Castrucci, S.; Josey, D. S.; Lu, Z.; Bender, T. P. Assessing the Potential Roles of Silicon and Germanium Phthalocyanines in Planar Heterojunction Organic Photovoltaic Devices and How Pentafluoro Phenoxylation Can Enhance π-π Interactions and Device Performance. *ACS Appl. Mater. Interfaces* **2015**, *7* (9), 5076−5088.
(17) Melville, O. A.; Grant, T. M.; Mirka, B.; Boileau, N. T.; Park, J.; Lessard, B. H. Ambipolarity and Air Stability of Silicon Phthalocyanine Organic Thin-Film Transistors. *Adv. Electron. Mater.* **2019**, *5* (8), 1900087.
(18) Melville, O. A.; Grant, T. M.; Lessard, B. H. Silicon Phthalocyanines as N-Type Semiconductors in Organic Thin Film Transistors. *J. Mater. Chem. C* **2018**, *6* (20), 5482−5488.
(19) Lessard, B. H.; Grant, T. M.; White, R.; Thibau, E.; Lu, Z.; Bender, T. P. The Position and Frequency of Fluorine Atoms Changes the Electron Donor/Acceptor Properties of Fluorophenoxy Silicon Phthalocyanines within Organic Photovoltaic Devices. *J. Mater. Chem. A* **2015**, *3* (48), 24512−24524.
(20) Raboui, H.; Lough, A. J.; Plint, T.; Bender, T. P. Position of Methyl and Nitrogen on Axial Aryloxy Substituents Determines the Crystal Structure of Silicon Phthalocyanines. *Cryst. Growth Des.* **2018**, *18* (5), 3193−3201.
(21) Lessard, B. H.; Lough, A. J.; Bender, T. P. Crystal Structures of Bis (Phenoxy) Silicon Phthalocyanines: Increasing p - p Interactions, Solubility and Disorder and No Halogen Bonding Observed Research Communications. *Acta Crystallogr. E* **2016**, *72* (E72), 988−994.
(22) King, B.; Daszczynski, A.; Rice, N.; Peltekoff, A. J.; Yutronkie, N.; Lessard, B.; Brusso, J. Cyanophenoxy-Substituted Silicon Phthalocyanines for Low Threshold Voltage n-Type Organic Thin-Film Transistors. *ACS Appl. Electron. Mater.* **2021**, *3* (5), 2212−2223.
(23) Vebber, M. C.; Grant, T. M.; Brusso, J. L.; Lessard, B. H. Bis (Trialkylsilyl Oxide) Silicon Phthalocyanines: Understanding the Role of Solubility in Device Performance as Ternary Additives in Organic Photovoltaics. *Langmuir* **2020**, *36* (10), 2612−2621.
(24) Grant, T. M.; Dindault, C.; Rice, N. A.; Swaraj, S.; Lessard, B. H. Synthetically Facile Organic Solar Cells with > 4% Efficiency Using P3HT and a Silicon Phthalocyanine Non-Fullerene Acceptor. *Mater. Adv.* **2021**, *2* (8), 2594−2599.
(25) Lessard, B. H.; Dang, J. D.; Grant, T. M.; Gao, D.; Seferos, D.; Bender, T. P. Bis(Tri-n-Hexylsilyl Oxide) Silicon Phthalocyanine: A Unique Additive in Ternary Bulk Heterojunction Organic Photovoltaic Devices. *ACS Appl. Mater. Interfaces* **2014**, *6* (17), 15040−15051.
(26) Grant, T. M.; Gorisse, T.; Dautel, O. J.; Wantz, G.; Lessard, B. H. Multifunctional Ternary Additive in Bulk Heterojunction OPV: Increased Device Performance and Stability. *J. Mater. Chem. A* **2017**, *5* (4), 1581−1587.
(27) Zysman-Colman, E.; Ghosh, S. S.; Xie, G.; Varghese, S.; Chowdhury, M.; Sharma, N.; Cordes, D. B.; Slawin, A. M. Z.; Samuel, I. D. W. Solution-Processable Silicon Phthalocyanines in Electroluminescent and Photovoltaic Devices. *ACS Appl. Mater. Interfaces* **2016**, *8* (14), 9247−9253.
(28) Ke, L.; Min, J.; Adam, M.; Gasparini, N.; Hou, Y.; Perea, J. D.; Chen, W.; Zhang, H.; Fladischer, S.; Sale, A.; Spiecker, E.; Tykwinski, R. R.; Brabec, C. J.; Ameri, T. A Series of Pyrene-Substituted Silicon Phthalocyanines as Near-IR Sensitizers in Organic Ternary Solar Cells. *Adv. Energy Mater.* **2016**, *6* (7), 1502355.
(29) Ke, L.; Gasparini, N.; Min, J.; Zhang, H.; Adam, M.; Rechberger, S.; Forberich, K.; Zhang, C.; Spiecker, E.; Tykwinski, R. R.; Brabec, C. J.; Ameri, T. Panchromatic Ternary/Quaternary Polymer/Fullerene BHJ Solar Cells Based on Novel Silicon Naphthalocyanine and Silicon Phthalocyanine Dye Sensitizers. *J. Mater. Chem. A* **2017**, *5* (6), 2550−2562.
(30) Mitra, K.; Hartman, M. C. T. Silicon Phthalocyanines: Synthesis and Resurgent Applications. *Org. Biomol. Chem.* **2021**, *19*, 1168−1190.
(31) Joyner, R. D.; Cekada, J., Jr; Linck, R. G.; Kenney, M. E. Diphenoxysilicon Phthalocyanine. *J. Inorg. Nucl. Chem.* **1960**, *15* (3−4), 387−388.
(32) Grant, T. M.; Rice, N. A.; Muccioli, L.; Castet, F.; Lessard, B. H. Solution-Processable n-Type Tin Phthalocyanines in Organic Thin Film Transistors and as Ternary Additives in Organic Photovoltaics. *ACS Appl. Electron. Mater.* **2019**, *1* (4), 494−504.
(33) Cranston, R.; Vebber, M.; Rice, N.; Tonnelé, C.; Castet, F.; Muccioli, L.; Brusso, J.; Lessard, B. N-Type Solution-Processed Tin versus Silicon Phthalocyanines: Improved Organic Thin Film Transistors but Unfavourable in Organic Photovoltaics. *ACS Appl. Electron. Mater.* **2021**, *3* (4), 1873−1885.
(34) Barrett, P. A.; Dent, C. E.; Linstead, R. P. 382. Phthalocyanines. Part VII. Phthalocyanine as a Co-Ordinating Group. A General Investigation of the Metallic Derivatives. *J. Chem. Soc.* **1936**, 1719−1736.
(35) Lowery, M. K.; Starshak, A. J.; Esposito, J. N.; Krueger, P. C.; Kenney, M. E. Dichloro(Phthalocyanino)Silicon. *Inorg. Chem.* **1965**, *4*, 128.
(36) Yutronkie, N. J.; Grant, T. M.; Melville, O. A.; Lessard, B. H.; Brusso, J. L. Old Molecule, New Chemistry: Exploring Silicon Phthalocyanines as Emerging N-Type Materials in Organic Electronics. *Materials* **2019**, *12* (8), 1334.
(37) Grant, T. M.; McIntyre, V.; Vestfrid, J.; Raboui, H.; White, R. T.; Lu, Z.-H.; Lessard, B. H.; Bender, T. P. Straightforward and Relatively Safe Process for the Fluoride Exchange of Trivalent and Tetravalent Group 13 and 14 Phthalocyanines. *ACS Omega* **2019**, *4* (3), 5317−5326.
(38) Dang, M.; Grant, T. M.; Yan, H.; Seferos, D.; Lessard, B. H.; Bender, T. P. Bis(Tri-n-Alkylsilyl Oxide) Silicon Phthalocyanines: A Start to Establishing a Structure Property Relationship as Both Ternary Additives and Nonfullerene Electron Acceptors in Bulk Heterojunction Organic Photovoltaic Devices. *J. Mater. Chem. A* **2017**, *5* (24), 12168−12182.
(39) Abdulrazzaq, O. A.; Saini, V.; Bourdo, S.; Dervishi, E.; Biris, A. S. Organic Solar Cells: A Review of Materials, Limitations, and Possibilities for Improvement. *Part. Sci. Technol.* **2013**, *31* (5), 427−442.
(40) Eftaiha, A. F.; Sun, J.-P.; Hill, I. G.; Welch, G. C. Recent Advances of Non-Fullerene, Small Molecular Acceptors for Solution Processed Bulk Heterojunction Solar Cells. *J. Mater. Chem. A* **2014**, *2* (5), 1201−1213.
(41) Branston, R.; Duff, J.; Hsiao, C. K.; Loutfy, R. O. *Photovoltaic Properties of Organic Photoactive Particle Dispersions: Polymeric Phthalocyanines*; ACS Symposium Series, Vol. *220*; American Chemical Society, 1983. DOI: 10.1021/bk-1983-0220.ch027.
(42) Honda, S.; Nogami, T.; Ohkita, H.; Benten, H.; Ito, S. Improvement of the Light-Harvesting Efficiency in Polymer/Fullerene Bulk Heterojunction Solar Cells by Interfacial Dye Modification. *ACS Appl. Mater. Interfaces* **2009**, *1* (4), 804−810.
(43) Ito, S.; Ohkita, H.; Benten, H.; Honda, S. Spectroscopic Analysis of NIR-Dye Sensitization in Bulk Heterojunction Polymer Solar Cells. *Ambio* **2012**, *41* (S2), 132−134.
(44) Honda, S.; Yokoya, S.; Ohkita, H.; Benten, H.; Ito, S. Light-Harvesting Mechanism in Polymer/Fullerene/Dye Ternary Blends Studied by Transient Absorption Spectroscopy. *J. Phys. Chem. C* **2011**, *115* (22), 11306−11317.
(45) Honda, S.; Ohkita, H.; Benten, H.; Ito, S. Selective Dye Loading at the Heterojunction in Polymer/Fullerene Solar Cells. *Adv. Energy Mater.* **2011**, *1* (4), 588−598.
(46) Xu, H.; Ohkita, H.; Tamai, Y.; Benten, H.; Ito, S. Interface Engineering for Ternary Blend Polymer Solar Cells with a Heterostructured Near-IR Dye. *Adv. Mater.* **2015**, *27* (39), 5868−5874.
(47) Grant, T. M.; Kaller, K. L. C.; Coathup, T. J.; Rice, N. A.; Hinzer, K.; Lessard, B. H. High Voc Solution-Processed Organic Solar Cells Containing Silicon Phthalocyanine as a Non-Fullerene Electron Acceptor. *Org. Electron.* **2020**, *87*, 105976.
(48) Vebber, M.; Rice, N. A.; Brusso, J. L.; Lessard, B. H. High Voc Fullerene-Free Organic Photovoltaics Composed of PTB7 and Axially-Substituted Silicon Phthalocyanines. *Sci. Rep.* **2021**, submitted for publication.
(49) Andersen, T. R.; Weyhe, A. T.; Tao, Q.; Zhao, F.; Qin, R.; Zhang, S.; Chen, H.; Yu, D. Novel Cost-Effective Acceptor: P3HT Based

Organic Solar Cells Exhibiting the Highest Ever Reported Industrial Readiness Factor. *Mater. Adv.* **2020**, *1* (4), 658−665.
(50) Du, X.; Heumueller, T.; Gruber, W.; Classen, A.; Unruh, T.; Li, N.; Brabec, C. J. Efficient Polymer Solar Cells Based on Non-Fullerene Acceptors with Potential Device Lifetime Approaching 10 Years. *Joule* **2019**, *3* (1), 215−226.
(51) Brabec, C. J.; Distler, A.; Du, X.; Egelhaaf, H.; Hauch, J.; Heumueller, T.; Li, N. Material Strategies to Accelerate OPV Technology toward a GW Technology. *Adv. Energy Mater.* **2020**, *10* (43), 2001864.
(52) Faure, M. D. M.; Grant, T. M.; Lessard, B. H. Silicon Phthalocyanines as Acceptor Candidates in Mixed Solution/Evaporation Processed Planar Heterojunction Organic Photovoltaic Devices. *Coatings* **2019**, *9* (3), 203.
(53) Lim, B.; Margulis, G. Y.; Yum, J.-H.; Unger, E. L.; Hardin, B. E.; Graetzel, M.; McGehee, M. D.; Sellinger, A. Silicon-Naphthalo/Phthalocyanine-Hybrid Sensitizer for Efficient Red Response in Dye-Sensitized Solar Cells. *Org. Lett.* **2013**, *15* (4), 784−787.
(54) Paterson, A. F.; Singh, S.; Fallon, K. J.; Hodsden, T.; Han, Y.; Schroeder, B. C.; Bronstein, H.; Heeney, M.; McCulloch, I.; Anthopoulos, T. D. Recent Progress in High-mobility Organic Transistors: A Reality Check. *Adv. Mater.* **2018**, *30* (36), 1801079.
(55) Kumar, B.; Kaushik, B. K.; Negi, Y. S. Perspectives and Challenges for Organic Thin Film Transistors: Materials, Devices, Processes and Applications. *J. Mater. Sci.: Mater. Electron.* **2014**, *25* (1), 1−30.
(56) Brixi, S.; Melville, O. A.; Mirka, B.; He, Y.; Hendsbee, A. D.; Meng, H.; Li, Y.; Lessard, B. H. Air and Temperature Sensitivity of n-Type Polymer Materials to Meet and Exceed the Standard of N2200. *Sci. Rep.* **2020**, *10* (1), 4014.
(57) Li, Y.; Sonar, P.; Murphy, L.; Hong, W. High Mobility Diketopyrrolopyrrole (DPP)-Based Organic Semiconductor Materials for Organic Thin Film Transistors and Photovoltaics. *Energy Environ. Sci.* **2013**, *6* (6), 1684−1710.
(58) Mirka, B.; Rice, N. A.; Williams, P.; Tousignant, M. N.; Boileau, N. T.; Bodnaryk, W. J.; Fong, D.; Adronov, A.; Lessard, B. H. Excess Polymer in Single-Walled Carbon Nanotube Thin-Film Transistors: Its Removal Prior to Fabrication Is Unnecessary. *ACS Nano* **2021**, *15* (5), 8252−8266.
(59) Rice, N. A.; Bodnaryk, W. J.; Mirka, B.; Melville, O. A.; Adronov, A.; Lessard, B. H. Polycarbazole-Sorted Semiconducting Single-Walled Carbon Nanotubes for Incorporation into Organic Thin Film Transistors. *Adv. Electron. Mater.* **2019**, *5* (1), 1800539.
(60) Mirka, B.; Fong, D.; Rice, N. A.; Melville, O. A.; Adronov, A.; Lessard, B. H. Polyfluorene-Sorted Semiconducting Single-Walled Carbon Nanotubes for Applications in Thin-Film Transistors. *Chem. Mater.* **2019**, *31* (8), 2863−2872.
(61) Quinn, J. T. E.; Zhu, J.; Li, X.; Wang, J.; Li, Y. Recent Progress in the Development of N-Type Organic Semiconductors for Organic Field Effect Transistors. *J. Mater. Chem. C* **2017**, *5* (34), 8654−8681.
(62) Dou, J.; Zheng, Y.; Yao, Z.; Lei, T.; Shen, X.; Luo, X.; Yu, Z.; Zhang, S.; Han, G.; Wang, Z.; et al. A Cofacially Stacked Electron-Deficient Small Molecule with a High Electron Mobility of over 10 cm^2 V^{-1} S^{-1} in Air. *Adv. Mater.* **2015**, *27* (48), 8051−8055.
(63) Dou, J.-H.; Zheng, Y.-Q.; Yao, Z.-F.; Yu, Z.-A.; Lei, T.; Shen, X.; Luo, X.-Y.; Sun, J.; Zhang, S.-D.; Ding, Y.-F.; et al. Fine-Tuning of Crystal Packing and Charge Transport Properties of BDOPV Derivatives through Fluorine Substitution. *J. Am. Chem. Soc.* **2015**, *137* (50), 15947−15956.
(64) Zhang, C.; Zang, Y.; Gann, E.; McNeill, C. R.; Zhu, X.; Di, C.; Zhu, D. Two-Dimensional π-Expanded Quinoidal Terthiophenes Terminated with Dicyanomethylenes as n-Type Semiconductors for High-Performance Organic Thin-Film Transistors. *J. Am. Chem. Soc.* **2014**, *136* (46), 16176−16184.
(65) Zhang, C.; Zang, Y.; Zhang, F.; Diao, Y.; McNeill, C. R.; Di, C.; Zhu, X.; Zhu, D. Pursuing High-Mobility N-Type Organic Semiconductors by Combination of"" ""Molecule-Framework""" and""" ""Side-Chain""" Engineering. *Adv. Mater.* **2016**, *28* (38), 8456−8462.
(66) King, B.; Melville, O. A.; Rice, N. A.; Kashani, S.; Tonnelé, C.; Raboui, H.; Swaraj, S.; Grant, T. M.; McAfee, T.; Bender, T. P.; et al. Silicon Phthalocyanines for n-Type Organic Thin-Film Transistors: Development of Structure−Property Relationships. *ACS Appl. Electron. Mater.* **2021**, *3* (1), 325−336.
(67) Melville, O. A.; Grant, T. M.; Lochhead, K.; King, B.; Ambrose, R.; Rice, N. A.; Boileau, N. T.; Peltekoff, A. J.; Tousignant, M.; Hill, I. G.; Lessard, B. H. Contact Engineering Using Manganese, Chromium, and Bathocuproine in Group 14 Phthalocyanine Organic Thin-Film Transistors. *ACS Appl. Electron. Mater.* **2020**, *2* (5), 1313−1322.
(68) Gali, S. M.; Matta, M.; Lessard, B. H.; Castet, F.; Muccioli, L. Ambipolarity and Dimensionality of Charge Transport in Crystalline Group 14 Phthalocyanines: A Computational Study. *J. Phys. Chem. C* **2018**, *122* (5), 2554−2563.
(69) Cranston, R. R.; Vebber, M. C.; Berbigier, J. F.; Rice, N. A.; Tonnelé, C.; Comeau, Z. J.; Boileau, N. T.; Brusso, J. L.; Shuhendler, A. J.; Castet, F.; Muccioli, L.; Kelly, T. L.; Lessard, B. H. Thin-Film Engineering of Solution-Processable n-Type Silicon Phthalocyanines for Organic Thin-Film Transistors. *ACS Appl. Mater. Interfaces* **2021**, *13* (1), 1008−1020.
(70) Pearson, A. J.; Plint, T.; Jones, S. T. E.; Lessard, B. H.; Credgington, D.; Bender, T. P.; Greenham, N. C. Silicon Phthalocyanines as Dopant Red Emitters for Efficient Solution Processed OLEDs. *J. Mater. Chem. C* **2017**, *5* (48), 12688−12698.
(71) Plint, T.; Lessard, B. H.; Bender, T. P. Assessing the Potential of Group 13 and 14 Metal/Metalloid Phthalocyanines as Hole Transport Layers in Organic Light Emitting Diodes. *J. Appl. Phys.* **2016**, *119* (14), 145502.
(72) Bonardi, A. H.; Dumur, F.; Grant, T. M.; Noirbent, G.; Gigmes, D.; Lessard, B. H.; Fouassier, J.-P.; Lalevée, J. High Performance Near-Infrared (NIR) Photoinitiating Systems Operating under Low Light Intensity and in the Presence of Oxygen. *Macromolecules* **2018**, *51* (4), 1314−1324.
(73) Bonardi, A.-H.; Bonardi, F.; Morlet-Savary, F.; Dietlin, C.; Noirbent, G.; Grant, T. M.; Fouassier, J.-P.; Dumur, F.; Lessard, B. H.; Gigmes, D.; Lalevee, J. Photoinduced Thermal Polymerization Reactions. *Macromolecules* **2018**, *51* (21), 8808−8820.
(74) Li, K.; Qiu, L.; Liu, Q.; Lv, G.; Zhao, X.; Wang, S.; Lin, J. Conjugate of Biotin with Silicon (IV) Phthalocyanine for Tumor-Targeting Photodynamic Therapy. *J. Photochem. Photobiol., B* **2017**, *174*, 243−250.
(75) Master, A. M.; Livingston, M.; Oleinick, N. L.; Sen Gupta, A. Optimization of a Nanomedicine-Based Silicon Phthalocyanine 4 Photodynamic Therapy (Pc 4-PDT) Strategy for Targeted Treatment of EGFR-Overexpressing Cancers. *Mol. Pharmaceutics* **2012**, *9* (8), 2331−2338.
(76) Hutnick, M. A.; Ahsanuddin, S.; Guan, L.; Lam, M.; Baron, E. D.; Pokorski, J. K. PEGylated Dendrimers as Drug Delivery Vehicles for the Photosensitizer Silicon Phthalocyanine Pc 4 for Candidal Infections. *Biomacromolecules* **2017**, *18* (2), 379−385.
(77) Baron, E. D.; Malbasa, C. L.; Santo-Domingo, D.; Fu, P.; Miller, J. D.; Hanneman, K. K.; Hsia, A. H.; Oleinick, N. L.; Colussi, V. C.; Cooper, K. D. Silicon Phthalocyanine (pc 4) Photodynamic Therapy Is a Safe Modality for Cutaneous Neoplasms: Results of a Phase 1 Clinical Trial. *Lasers Surg. Med.* **2010**, *42* (10), 888−895.
(78) Lam, M.; Dimaano, M. L.; Oyetakin-White, P.; Retuerto, M. A.; Chandra, J.; Mukherjee, P. K.; Ghannoum, M. A.; Cooper, K. D.; Baron, E. D. Silicon Phthalocyanine 4 Phototoxicity in Trichophyton Rubrum. *Antimicrob. Agents Chemother.* **2014**, *58* (6), 3029−3034.
(79) Galstyan, A.; Schiller, R.; Dobrindt, U. Boronic Acid Functionalized Photosensitizers: A Strategy to Target the Surface of Bacteria and Implement Active Agents in Polymer Coatings. *Angew. Chem., Int. Ed.* **2017**, *56* (35), 10362−10366.
(80) Li, K.; Dong, W.; Liu, Q.; Lv, G.; Xie, M.; Sun, X.; Qiu, L.; Lin, J. A Biotin Receptor-Targeted Silicon (IV) Phthalocyanine for in Vivo Tumor Imaging and Photodynamic Therapy. *J. Photochem. Photobiol., B* **2019**, *190*, 1−7.
(81) Mitsunaga, M.; Ogawa, M.; Kosaka, N.; Rosenblum, L. T.; Choyke, P. L.; Kobayashi, H. Cancer Cell-Selective in Vivo near

https://doi.org/10.1021/acsami.1c06060
ACS Appl. Mater. Interfaces 2021, 13, 31321−31330

Infrared Photoimmunotherapy Targeting Specific Membrane Molecules. *Nat. Med.* **2011**, *17* (12), 1685−1691.

https://doi.org/10.1021/acsami.1c06060
ACS Appl. Mater. Interfaces 2021, 13, 31321−31330